Bulletin of the Seismological Society of America, Vol. 99, No. 1, pp. 416–421, February 2009, doi: 10.1785/0120080120

Short Note

Pn Travel-Time Tomography of the Paleo-Continental-Collision and Rifting Zone around Korea and Japan

by Tae-Kyung Hong and Tae-Seob Kang

Abstract A recent dense deployment of seismic stations in South Korea and Japan allows regional seismic imaging of the far-east Asian region that experienced continental collisions and riftings. We perform seismic imaging based on a mantle-lid *P*-wave (*Pn*) travel-time tomography to exploit the tectonic imprints in the lithosphere. The average *Pn* velocity in the region is estimated to be 7.95 ± 0.03 km/sec. The inverted *Pn* velocities illuminate the tectonic structures. High velocities of ~8.15 km/sec are observed in the Precambrian massif regions, while low velocities of ~7.8 km/sec are associated with the fold belt and sedimentary basin regions in the southern Korean Peninsula. The *Pn* velocity is estimated to be low in the backarc basins, including the Ulleung and the Yamato basins, while it is estimated to be higher on the continental fragments, including the South Korea plateau and the Oki bank. The high-velocity structures along the Japanese Islands support the separation of the Japanese province from the Eurasia plate. The high-velocity anomaly along the east coast of the Korean Peninsula around the Hupo bank suggests intrusion and solidification of high-density material in the lower crust and mantle lid.

Introduction

The far-east Asian region (northwestern Pacific), including the Korean Peninsula, the East Sea (Sea of Japan), and Japan, experienced complex tectonic evolutions, which are not yet fully understood despite various efforts (e.g., Kimura and Tamaki, 1986; Lallemand and Jolivet, 1986; Lee *et al.*, 1999). Some outstanding tectonic questions are the evolution of the East Sea and the Korean Peninsula in their current shapes and their tectonic relationships.

Seismic velocities generally vary with the lithology and rheology of the medium, which can be interpreted in terms of constituent materials, temperature, and pressure (e.g., Trampert *et al.*, 2001). A tectonic evolution accompanies high-energy exertion on the medium, causing anisotropic perturbation in the medium. The imprinted tectonic signatures and perturbations of the medium are slowly healed with geological time, causing an increase of seismic velocities with the geological age of the medium (e.g., Li *et al.*, 1998; Ritsema and van Heijst, 2000). Thus, historical tectonic evolution can be inferred from the seismic velocities of a medium.

It is known that the East Sea was opened due to continental rifting during the Oligocene and Miocene periods. The continental rifting that typically accompanies lithospheric deformation can be investigated by examining the medium properties in the lower crust and mantle lid. The seismic phase *Pn* is the regional *P* phase traveling through the mantle lid. The *Pn* phase is, thus, useful for studying the properties in the Moho and uppermost mantle. In this study, we perform a *Pn* travel-time tomography around the Korean Peninsula, the East Sea, and Japan. The *Pn* velocities in the Korean Peninsula and the East Sea have not been previously studied. We discuss the tectonic implications of the tomography results.

Tectonic and Geological Structures

The lithospheric tectonic structure of the Korean Peninsula is composed of three Precambrian massif blocks (i.e, Nangnim, Gyeonggi, and Yeongnam). There are two fold belts (i.e., Imjingang and Okcheon) intervening between the massif blocks (Fig. 1). The presence of the intervening fold belts suggests sutures and/or collisions between massif blocks (Fitches *et al.*, 1991; Yin and Nie, 1993; Liou *et al.*, 1994; Chough *et al.*, 2000). It is known that the unification of the three massif blocks into the current shape was completed during the Jurassic period (Chough *et al.*, 2000).

A sedimentary basin called the Gyeongsang basin is located in the southeastern margin of the peninsula. The Gyeongsang basin was formed in the Cretaceous period. The presence of volcanic sediments suggests that the Gyeongsang basin developed as a result of subduction. In the Cre-

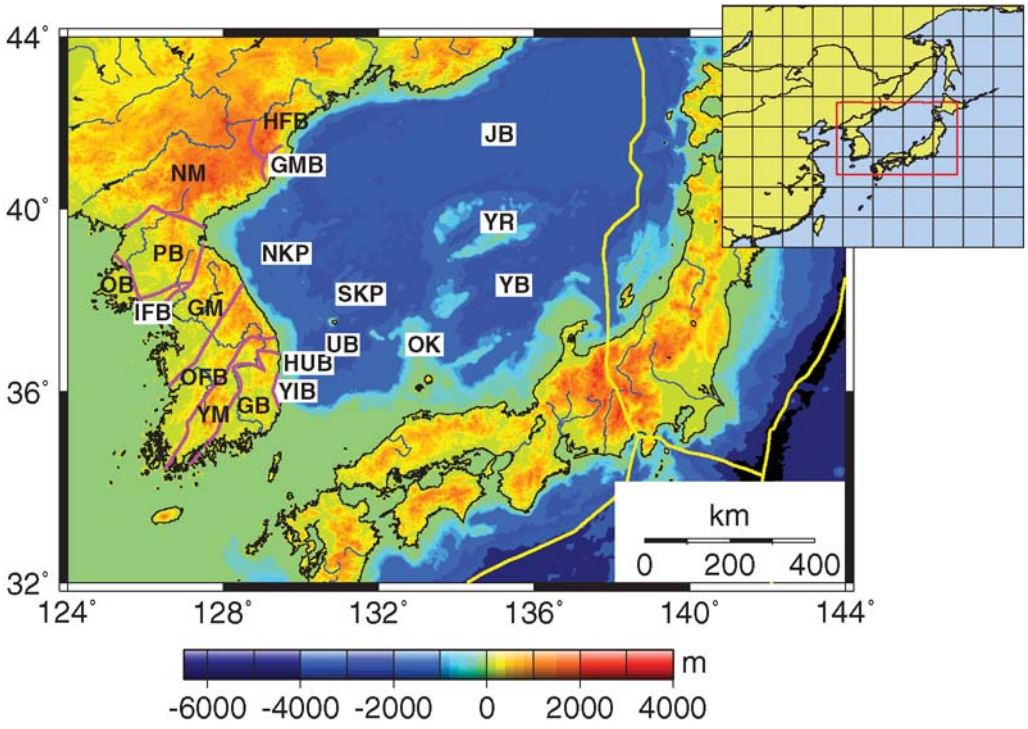

Figure 1. Map of geology. Major tectonic structures are denoted: Gyeongsang basin, GB; Gyeongsang massif, GM; Gilju-Myeongcheon basin, GMB; Hambuk fold belt, HFB; Hupo bank and basin, HUB; Imjingang fold belt, IFB; Japan basin, JB; North Korea plateau, NKP; Nangnim massif, NM; Ongjin basin, OB; Okcheon fold belt, OFB; Oki bank, OK; Pyeongnam basin, PB; South Korea plateau, SKP; Ulleung basin, UB; Yamato basin, YB; Yeonil basin, YIB; Yeongnam massif, YM; and Yamato rise, YR.

taceous period, the westward subduction of the paleo-Izanagi plate beneath the eastern margin of the Eurasia plate caused widespread volcanic activity in the southeastern Korean Peninsula (Chough *et al.*, 2000).

The opening of the East Sea started in the Oligocene and was completed in the mid-Miocene. It is known that the India–Eurasia plate collision and successive microplate rotations served as the driving force for the opening in the East Sea (Kimura and Tamaki, 1986). Several mechanisms were proposed for explanation of the East Sea opening (e.g., the fan-shaped rotational opening model, Otofuji *et al.* [1985], the pull-apart model, Jolivet *et al.* [1994]). However, many aspects still remain unclear. The Japanese Islands were separated from the Eurasia plate due to the East Sea opening. The East Sea is composed of three deep-seated backarc basins (i.e, Japan, Yamato, and Ulleung). The East Sea has experienced the east–west directed compression since the mid-Miocene, which is responsible for the seismicity of the eastern margin of the East Sea (Jolivet and Huchon, 1989).

Data

We collected seismic travel-time data for regional events with focal depths less than 35 km, which occurred around the Korean Peninsula and Japanese Islands during 2000–2007. The total number of events is 97 (Fig. 2a). The magnitudes of events collected around the Korean Peninsula are greater than 3.3, and the magnitude of those collected around the Japanese Islands are greater than 6.0. The seismic data were recorded by broadband and short-period stations deployed in South Korea, Japan, and China. The total number of stations used in this study is 168, yielding 5244 regional seismic records. The event information is collected from the event catalogs of the International Seismological Centre (ISC) and local seismological bureaus. The epicentral distances are between 180 and 1900 km.

Good ray path coverage is observed in most regions of southern Korea, the East Sea, and the Japanese Islands (Fig. 2b). The azimuthal distribution of ray paths on the East Sea is observed to be clustered in a narrow azimuthal range, which does not allow us to assess the azimuth-dependent *Pn* velocity. We invert for azimuthally averaged *Pn* velocity.

Method and Processing

The *Pn* travel time in a discretized medium can be expressed by (e.g., Hearn, 1996)

$$t_{ij} = a_i + b_j + \sum d_{ijk} s_k, \tag{1}$$

where a_i is the static delay for station i, b_j is the static delay for event j, t_{ij} is the *Pn* travel time for the pair of station i and event j, d_{ijk} is the propagation distance in cell k along the ray path, and s_k is the *Pn* slowness (inverse velocity) in cell k. The set of equations from (1) is solved using the regularized

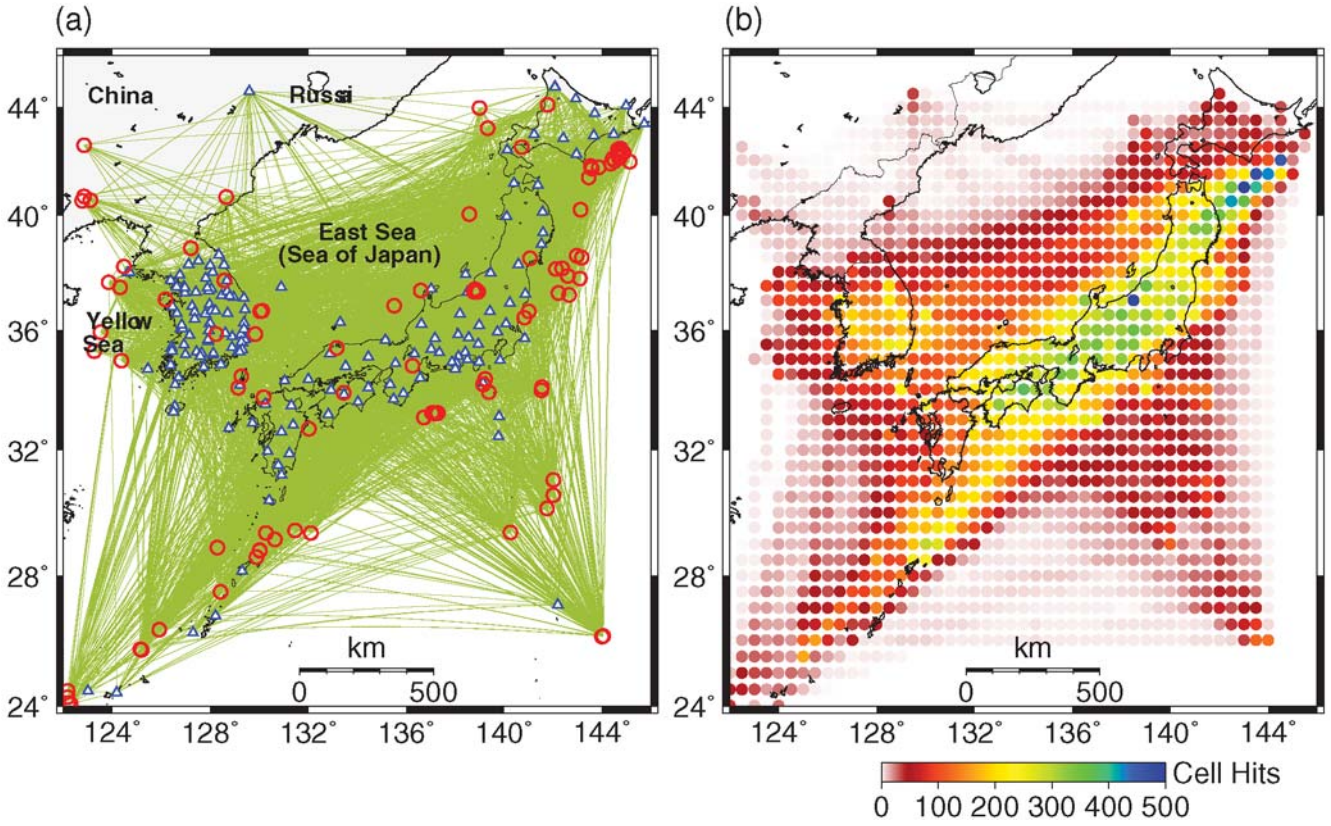

Figure 2. Locations of (a) events and stations and (b) the ray path density. The events are denoted by circles and the stations by triangles. The great-circle paths are presented with solid lines. The *Pn* ray path coverage is good within the southern Korean Peninsula, the East Sea, and the Japanese Islands.

least-squares QR (LSQR) factorization algorithm (Paige and Saunders, 1982). We iterate the inversion until the difference between successive solutions is smaller than a given criteria. We tested various damping parameters for the tomographic inversion. The damping parameter applied in this study is 0.01, which makes stable and fast convergence in the inversion.

The *Pn* arrival times in the regional seismograms are determined by examining every seismogram manually after calculation of theoretical arrival times based on a 1D crustal model (Chang and Baag, 2005). The average *Pn* velocity is estimated to be 7.95 km/sec with a standard deviation of 0.03 km/sec from the observed *Pn* travel times (Fig. 3), which is slower by ~0.1 km/sec than the typical *Pn* velocities in the continental lithosphere (Hearn *et al.*, 2004; Pei *et al.*, 2007). We invert for the *Pn* velocities from the *Pn* travel times using the LSQR method.

Resolution Test

In order to evaluate the spatial resolution and to choose the optimum cell size for *Pn* travel-time tomography, a series of checkerboard tests is performed. We consider a checkerboard model with a 3° × 3° alternating pattern of positive and negative slowness anomalies. The magnitudes of the slowness anomalies are ±0.03 sec/km. Synthetic travel times are computed for the source–receiver pairs of field observations. The synthetic travel times are inverted using the inversion method described in the Method and Processing section. The inversion is conducted for various cell sizes from 0.1° to 2.0° at every step of 0.1°.

In each inversion, we checked the cell-hit counts and root mean square (rms) error reduction. Here, the rms error reduction is measured by $1 - \sqrt{\sum_{i=1}^{N}(t_i^p - t_i^o)/N}$, where t_i^o is the input travel time for ray path i, t_i^p is the recomputed travel time for the inverted slowness model, and N is the number of ray paths. We find that a cell size of 0.5° with average cell hits of 54 is the optimum cell size for our data set, yielding reasonable recovery of the checkerboard model (Fig. 4). We, thus, perform the travel-time inversion of field observations on a medium discretized with 0.5° × 0.5° cells. We display the regions with cell-hit counts of 50 or more for final presentation of the inverted model in this study.

Results

The estimated *Pn* velocity appears to be highly correlated with the tectonic structure (Fig. 5). High-velocity anomalies are observed in the massif regions (i.e., Nangnim, Gyeonggi, and Yeongnam). On the other hand, low-velocity

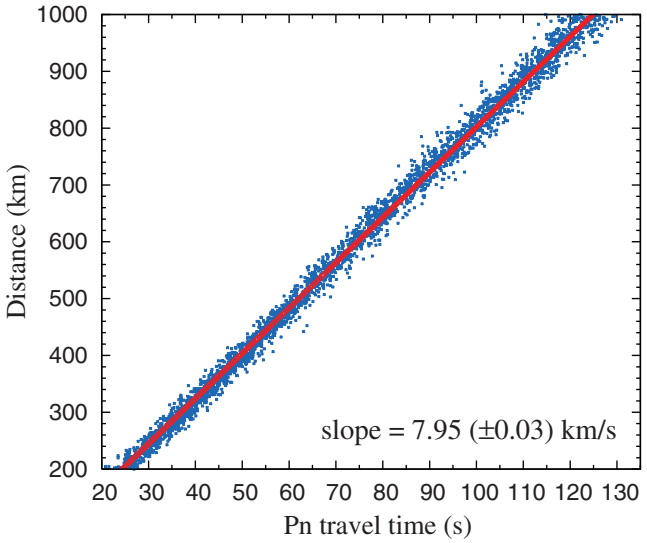

Figure 3. *Pn* travel times (5244) versus epicentral distances. The average *Pn* velocity is estimated to be 7.95 ± 0.03 km/sec over the study area, which is slower than the typical *Pn* velocity in the continental lithosphere.

anomalies are observed on the Okcheon fold belt region. The presence of a low-velocity structure in the Okcheon fold belt suggests that the continental collision during the Jurassic period incorporated lithospheric deformation. Also, the high-velocity anomalies illuminating the Gyeonggi and Yeongnam massifs appear to be shifted to the southeast. This observation suggests that the northern massif block (Gyeonggi) impinged beneath the southern massif block (Yeongnam) during the continental collision.

It is intriguing to note that a localized low-velocity anomaly is observed around 37° N and 127° E in the mantle lid of the Gyeonggi massif, which is consistent with a previous study (Kang and Shin, 2006). Also, we find a low-velocity structure developing along the eastern margin of the peninsula across the Gyeonggi massif, the Okcheon fold belt, and the Yeongnam massif. This low-velocity region corresponds to the Taebaek Mountain Range, which is the largest mountain range on the Korean Peninsula. The orogenic history responsible for the mountain range still remains unclear. The observation suggests that the orogeny developed after the unification of the massif blocks. The Yeonil basin in the southeastern margin of the Korean Peninsula is an observed high-velocity zone.

We also observe a north–south oriented high-velocity anomaly in the eastern offshore region of the Korean Peninsula. The location of the high-velocity anomaly corresponds to the Hupo bank and the South and North Korea plateaus. This agrees with the observation of a north–south elongated positive magnetic anomaly in the same region (Kim *et al.*, 2007). In addition, this feature is consistent with the observation of regional-phase attenuation in the eastern margin of the peninsula (Hong *et al.*, 2008). We observe low-velocity anomalies in the backarc basins (i.e., Yamato and Ulleung)

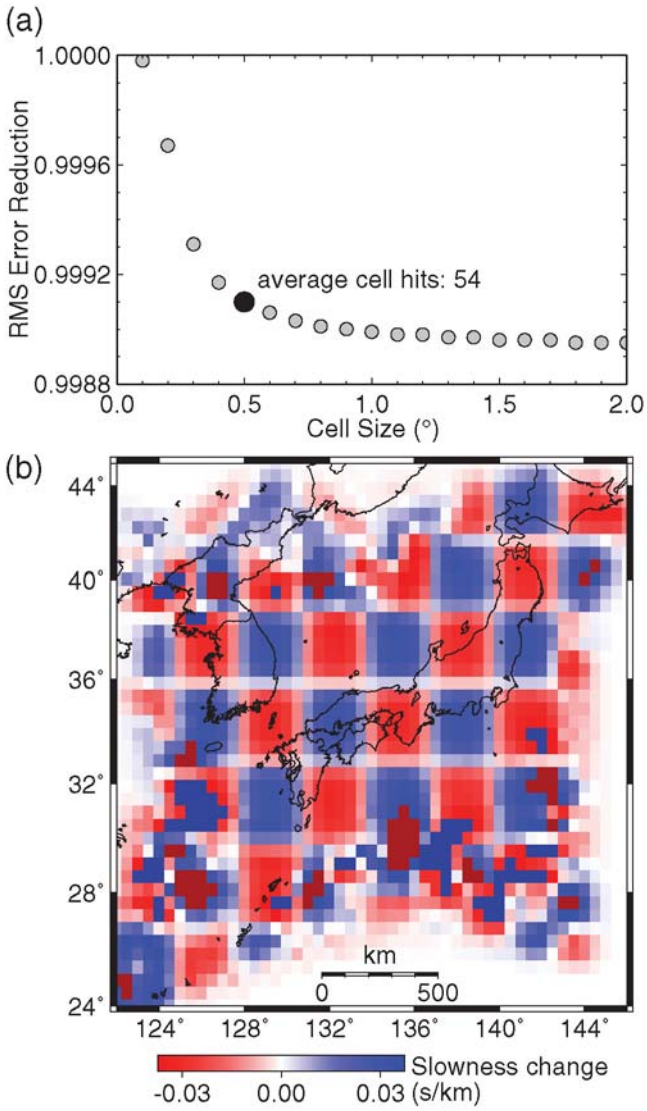

Figure 4. Spatial resolution test of the data set. (a) Variation of the rms error reduction with respect to the cell sizes from 0.1° to 2.0° with a uniform interval of 0.1°. High values of rms error reduction indicate a good match between input and recomputed travel times. Inversions based on small cell sizes produce high rms error reductions due to an increase in the degrees of freedom. The inverted models, however, do not agree well with the input model. Inversions based on large cell sizes, on the other hand, yield smeared features. The optimum cell size is determined to be 0.5° considering the trade-off relationship between the cell size and rms error reduction in the figure. The average cell-hit count for a medium discretized by 0.5° × 0.5° cells is 54. (b) The tomographic inversion based on cells with a size of 0.5° × 0.5° recovers well the checkerboard model in the regions with cell-hit counts of 50 or more.

and the Yamato rise. The low-velocity structure extends in a southwestern direction between the Korean Peninsula and the Japanese Islands. This geometry implies that the East Sea was opened in the northwest–southeast direction.

High-velocity structures spread over the Japanese Islands. The high-velocity structures are distributed not only on the mainlands but also on the eastern and western offshore

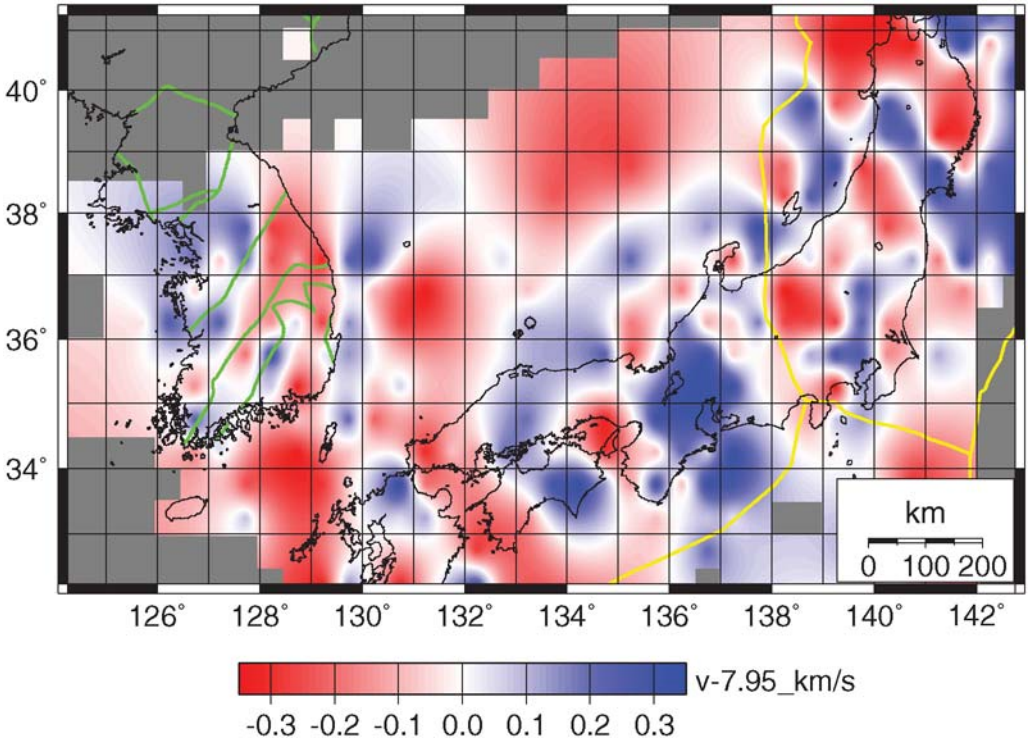

Figure 5. *Pn* travel-time tomography. The differential velocities relative to the reference *Pn* velocity (7.95 km/sec) are presented. Major tectonic structures are marked with solid lines. High-velocity anomalies are observed in the Precambrian massif regions, while slow-velocity anomalies are observed in the backarc basins. Localized low-velocity anomalies are observed on the Japanese Islands.

regions. The presence of high-velocity structures supports the tectonic history of continental separation between the Eurasia plate and the Japanese province during the East Sea opening. We also find localized low-velocity anomalies on the mainland of Japan. The low-velocity anomalies may be related to upwelling melts due to dehydration of subducting slabs beneath Japan (Zhao, 2001). The complex *Pn*-velocity structure in the Japanese Islands is consistent with previous studies (Hashida, 1989; Zhao *et al.*, 1990). In particular, high-seismic attenuation regions correlate with those of low velocities in this study.

Discussion and Conclusions

The tectonic structures in the far-east Asian region around Korea and Japan, which experienced complex tectonic evolutions such as continental rifting, collision, and orogeny, were studied using *Pn* travel-time tomography. The average *Pn* velocity in the study area is lower than that in the typical continental lithosphere, implying recent tectonic evolution of the region. The high- and low-velocity structures imaged by *Pn* travel-time tomography are highly correlated with known tectonic structures. The *Pn* velocity is estimated to be high in the Precambrian massif regions, while low in young tectonic regions (fold belts and backarc basins). The geometry of low-velocity anomalies in the East Sea reflects recent tectonic evolution with extension in a northeast–southwest direction.

It is noteworthy that the Yamato rise region is imaged as a low-velocity structure. This observation implies that the Yamato rise developed at a similar time to that of the Yamato basin formation. On the other hand, we find high-velocity anomalies associated with the continental fragments such as the South Korea plateau and the Oki bank. We also observe a north–south trending high-velocity anomaly off the east coast of the Korean Peninsula. This observation suggests intrusion of high-velocity materials in the lower crust and upper mantle, such as magma underplating (White and McKenzie, 1989; Cho *et al.*, 2004).

Data and Resources

Seismic waveform data and earthquake information used in this study were collected from the Web sites of the Korea Meteorological Administration (KMA, www.kma.go.kr, last accessed May 2008), the Korea Institute of Geoscience and Mineral Resources (KIGAM, quake.kigam.re.kr, last accessed May 2008), the International Seismic Centre (ISC, www.isc.ac.uk, last accessed May 2008), the Incorporated Research Institutions for Seismology (IRIS, www.iris.edu/data, last accessed May 2008), and the National Research Institute for Earth Science and Disaster Prevention (NIED, www.fnet.bosai.go.jp, last accessed May 2008). Some data were collected by visiting the institutes. Some figures were produced using the Generic Mapping

Tools (GMT, Wessel and Smith, 1998; gmt.soest.hawaii.edu, last accessed September 2007).

Acknowledgments

We are grateful to Korea Meteorological Administration (KMA), the Korea Institute of Geoscience and Mineral Resources (KIGAM), the Incorporated Research Institutions for Seismology (IRIS), and the National Research Institute for Earth Science and Disaster Prevention (NIED) in Japan for making seismic data available. We thank the associate editor, Diane Doser, and an anonymous reviewer for fruitful comments. This work was supported by the Korea Meteorological Administration Research and Development Program under Grant Number CATER 2007-5111.

References

Chang, S.-J., and C.-E. Baag (2005). Crustal structure in southern Korea from joint analysis of teleseismic receiver functions and surface-wave dispersion, *Bull. Seismol. Soc. Am.* **95,** no. 4, 1516–1534.

Cho, H.-M., H.-J. Kim, H.-T. Jou, J.-K. Hong, and C.-E. Baag (2004). Transition from rifted continental to oceanic crust at the southeastern Korean margin in the East Sea (Japan Sea), *Geophys. Res. Lett.* **31,** L07606, doi 10.1029/2003GL019107.

Chough, S. K., S.-T. Kwon, J.-H. Ree, and D. K. Choi (2000). Tectonic and sedimentary evolution of the Korean peninsula: a review and new view, *Earth Sci. Rev.* **52,** 175–235.

Fitches, W. R., C. J. N. Fletcher, and J. Xu (1991). Geotectonic relationships between cratonic blocks in E. China and Korea, *J. Southeast Asian Earth Sci.* **6,** 185–199.

Hashida, T. (1989). Three-dimensional seismic attenuation structure beneath the Japanese Islands and its tectonic and thermal implications, *Tectonophysics* **159,** 163–180.

Hearn, T. M. (1996). Anisotropic *Pn* tomography in the western United States, *J. Geophys. Res.* **101,** 8403–8414.

Hearn, T. M., S. Wang, J. F. Ni, Z. Xu, Y. Yu, and X. Zhang (2004). Uppermost mantle velocities beneath China and surrounding regions, *J. Geophys. Res.* **109,** B11301, doi 10.1029/2003JB002874.

Hong, T.-K., C.-E. Baag, H. Choi, and D.-H. Sheen (2008). Regional seismic observations of the October 9, 2006 underground nuclear explosion in North Korea and the influence of crustal structure on regional phases, *J. Geophys. Res.* **113,** B03305, doi 10.1029/2007JB004950.

Jolivet, L., and P. Huchon (1989). Crustal scale strike-slip deformation in Hokkaido, northeast Japan, *Struct. Geol.* **11,** 509–522.

Jolivet, L., K. Tamaki, and M. Fournier (1994). Japan Sea, opening history and mechanism: a synthesis, *J. Geophys. Res.* **99,** 22,237–22,259.

Kang, T.-S., and J. S. Shin (2006). Surface-wave tomography from ambient seismic noise of accelerograph networks in southern Korea, *Geophys. Res. Lett.* **33,** L17303, doi 10.1029/2006GL027044.

Kim, H.-J., G. H. Lee, H.-T. Jou, H.-M. Cho, H.-S. Yoo, G.-T. Park, and J.-S. Kim (2007). Evolution of the eastern margin of Korea: constraints on the opening of the East Sea (Japan Sea), *Tectonophysics* **436,** 37–55.

Kimura, G., and K. Tamaki (1986). Collision, rotation, and back-arc spreading in the region of the Okhotsk and Japan Seas, *Tectonics* **5,** 389–401.

Lallemand, S., and L. Jolivet (1986). Japan Sea: a pull-apart basin?, *Earth Planet. Sci. Lett.* **76,** 375–389.

Lee, Y. S., N. Ishikawa, and W. K. Kim (1999). Paleomagnetism of Tertiary rocks on the Korean Peninsula: tectonic implications for the opening of the East Sea (Sea of Japan), *Tectonophysics* **304,** 131–149.

Li, Y.-G., J. E. Vidale, K. Aki, F. Xu, and T. Burdette (1998). Evidence of shallow fault zone strengthening after the 1992 *M* 7.5 Landers, California, earthquake, *Science* **279,** 217–219.

Liou, J. G., R. Y. Zhang, and W. G. Ernst (1994). An introduction to ultrahigh-*P* metamorphism, *Isl. Arc* **3,** 1–24.

Otofuji, Y.-I., T. Matsuda, and S. Nohda (1985). Opening mode of the Japan Sea inferred from the palaeomagnetism of the Japan Arc, *Nature* **317,** 603–604.

Paige, C. C., and M. A. Saunders (1982). LSQR: an algorithm for sparse linear equations and sparse linear systems, *ACM Trans. Math. Softw.* **8,** 195–209.

Pei, S., J. Zhao, Y. Sun, Z. Xu, S. Wang, H. Liu, C. A. Rowe, M. N. Toksoz, and X. Gao (2007). Upper mantle seismic velocities and anisotropy in China determined through *Pn* and *Sn* tomography, *J. Geophys. Res.* **112,** B05312, doi 10.1029/2006JB004409.

Ritsema, J., and H. J. van Heijst (2000). A new model for the upper mantle structure beneath Africa, *Geology* **28,** 63–66.

Trampert, J., P. Vacher, and N. Vlaar (2001). Sensitivities of seismic velocities to temperature, pressure and composition in the lower mantle, *Phys. Earth Planet. Inter.* **124,** 255–267.

Wessel, P., and W. H. F. Smith (1998). New, improved version of the Generic Mapping Tools released, *Eos Trans. AGU*, **79,** 579.

White, R., and D. McKenzie (1989). Magmatism at rift zones: the generation of volcanic continental margins and flood basalts, *J. Geophys. Res.* **94,** no. B6, 7685–7729.

Yin, A., and S. Nie (1993). An indentation model for the north and south China collision and development of the Tan-Lu and Honam fault systems, eastern Asia, *Tectonics* **12,** 810–813.

Zhao, D. (2001). Seismological structure of subduction zones and its implications for arc magmatism and dynamics, *Phys. Earth Planet. Inter.* **127,** 197–214.

Zhao, D., S. Horiuchi, and A. Hasegawa (1990). 3-D seismic velocity structure of the crust and the uppermost mantle in the northeastern Japan Arc, *Tectonophysics* **181,** 135–149.

Department of Earth System Sciences
Yonsei University
Shinchon-dong, 134, Seodaemoon-gu
Seoul 120-749, South Korea
tkhong@yonsei.ac.kr
(T.-K.H.)

Earthquake Research Center
Korea Institute of Geoscience and Mineral Resources
Daejeon 305-350, South Korea
(T.-S.K.)

Manuscript received 3 June 2008